

# Application of Local Numerical Homogenization and *hp*-Adaptive FEM for Modeling of Heterogeneous Viscoelastic Materials

Marek KLIMCZAK, Witold CECOT

*Cracow University of Technology*

Warszawska 24, 31-155 Cracow, Poland

e-mail: mklimczak@L5.pk.edu.pl, plcecot@cyf-kr.edu.pl

In this paper the application of local numerical homogenization and *hp*-adaptive FEM for modeling of non-periodic heterogeneous viscoelastic materials is presented. These two methods were combined and modified in order to provide a novel tool for reliable and efficient analyses of structures made of the above mentioned materials. Short descriptions of both numerical methods as well as our approach are provided. Several numerical examples are presented in order to validate the effectiveness of the proposed method.

**Key words:** local numerical homogenization, *hp*-adaptive FEM, viscoelasticity.

## 1. INTRODUCTION

The reliable numerical modeling of heterogeneous materials plays a key role in analyses and design of many structures. Usually it is numerically impossible to account for every detail of the microstructure due to computational time limitations. In context of heterogeneous materials used in civil engineering one typically distinguishes two levels of analysis:

- microscale (mesoscale) that can be associated with the dimensions of the constituents,
- macroscale that can be associated with the overall structure size.

Bridging the mentioned scales in terms of numerical analysis can be performed in the way of various computational homogenization methods (e.g., [1–3]).

The asymptotic method proposed by BENSOUSSAN *et al.* [4] enables to compute homogenized material properties by a unit cell computation. The method was generalized for inelastic problems, e.g., by WIĘCKOWSKI [5].

GEERS *et al.* [1] proposed an approach based on representative volume elements (RVEs) which are very small subdomains fully accounting for the hetero-

geneous microstructure. The RVE analysis enables to calculate effective material operators at selected macroscale, typically Gauss integration points. For non-linear problems this procedure is iterative. The convergent stiffness matrix for an RVE enables determination of the tangent operator for a current Newton-Raphson iteration at the macroscale. Numerical analysis in both scales is performed using FEM.

MANG *et al.* [2] proposed the RVE-based method as well. Macroscale analysis is also performed using FEM but Mori-Tanaka method or generalized self-consistent schemes (both based on Eshelby's solution) are applied in order to calculate the effective material operators.

Contrary to those methods, Jhurani's approach [3], called local numerical homogenization, does not make use of the assumption that a considered composite has periodically varying properties and that the scales are separated, i.e.,

$$\frac{l}{L} \ll 1.0,$$

where  $l$  and  $L$  denote the micro and macroscale characteristic dimensions respectively. The Jhurani method will be presented in detail in further part of this paper.

Above mentioned methods enable to analyze the response of the structure made of heterogeneous materials transferring necessary information from the lower to the higher scale and significantly reducing computational time comparison to the 'brute force' solution.

Application of computational homogenization is even more urgent in the case of transient problems. Viscoelastic materials require such an approach. Thus, an incremental formulation at each time instant needs to be performed for an appropriate homogenization.

In our research we use the modified local numerical homogenization method, which does not require neither periodicity of the microstructure, nor the distinct separation of 'neighboring' scales. Modification of the original version of the method involves an updating of the load vector due to the inelastic strains evolution. At selected steps of the proposed approach we also use the *hp*-adaptive FEM in order to increase the effectiveness and reliability of the analysis. Preliminary numerical tests are presented in this paper.

## 2. PROBLEM FORMULATION

This paper is organized as follows. First we formulate the problem. Then, we present the local homogenization with our modifications. Finally, we present some benchmark results that illustrate possibilities of the proposed approach.

The strong formulation of the viscoelastic problem with Burgers constitutive equation is recapitulated below.

Find the displacements  $\mathbf{u}(\mathbf{x}, t)$  such that

$$(2.1) \quad \begin{cases} \operatorname{div} \dot{\boldsymbol{\sigma}} + \dot{\mathbf{X}} = 0 & \forall t, \mathbf{x} \in \omega_i \subset \Omega, \\ \dot{\boldsymbol{\sigma}} = \mathbf{C}[\dot{\boldsymbol{\varepsilon}}(\dot{\mathbf{u}}) - \dot{\boldsymbol{\varepsilon}}^*] & \forall t, \mathbf{x} \in \omega_i \subset \Omega, \\ \dot{\boldsymbol{\varepsilon}} = \frac{1}{2}[\nabla \dot{\mathbf{u}} + (\nabla \dot{\mathbf{u}})^T] & \forall t, \mathbf{x} \in \omega_i \subset \Omega, \\ \dot{\boldsymbol{\varepsilon}}^* = f(\boldsymbol{\sigma}, \boldsymbol{\chi}, \dots) & \forall t, \mathbf{x} \in \omega_i \subset \Omega, \\ + \text{initial, boundary,} \\ \& \text{continuity or debonding conditions,} \end{cases}$$

where dot above symbols denotes differentiation with respect to time and the following symbols are used:  $\boldsymbol{\sigma}$  – stress tensor,  $\mathbf{X}$  – body forces,  $\mathbf{C}$  – tensor of material parameters,  $\boldsymbol{\chi}$  – internal variable (inelastic strains in the case of Burgers model),  $\dot{\boldsymbol{\varepsilon}}^*$  – inelastic strain rate defined by Burgers model.

The basic mechanical representation of the Burgers constitutive model is shown in Fig. 1. Typically one uses the version with “ $N$ ” Kelvin-Voigt elements joined in a series.

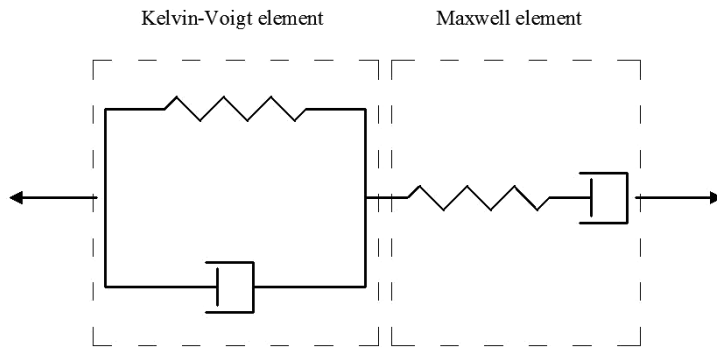


FIG. 1. Scheme of the 1D Burgers model.

Transforming the corresponding weak formulation of the problem (2.1) into the incremental form one obtains:

$$(2.2) \quad \int_{\Omega} \Delta \boldsymbol{\varepsilon} : {}^{t-\Delta t} \dot{\boldsymbol{\sigma}} d\omega = \int_{\Omega} \mathbf{v} \cdot \Delta \mathbf{X} d\omega + \int_{S_{\sigma}} \mathbf{v} \cdot \Delta \mathbf{t}^0 ds + \int_{\Omega} \Delta \boldsymbol{\varepsilon}^* : {}^{t-\Delta t} \dot{\boldsymbol{\sigma}} d\omega \quad \forall t, \forall \mathbf{v} \in H_0^1(\Omega),$$

where  $\mathbf{v}$  – test functions,  $\mathbf{t}^0$  – tractions,  ${}^{t-\Delta t}\dot{\boldsymbol{\sigma}}$  – stress rate field at time instant  $t - \Delta t$ ,  $H_0^1$  – the Sobolev space of the functions satisfying homogeneous Dirichlet boundary conditions.

The third term on the right-hand side is the inelastic extension to the load vector. It has to be computed iteratively at each time instant until the equilibrium is reached.

In the case of Burgers model the total strain increment ( $\Delta \boldsymbol{\varepsilon}$ ) can be decomposed into elastic ( $\Delta \boldsymbol{\varepsilon}_{el}$ ), viscous ( $\Delta \boldsymbol{\varepsilon}_v$ ) and viscoelastic ( $\Delta \boldsymbol{\varepsilon}_{ve}$ ) term as

$$(2.3) \quad \Delta \boldsymbol{\varepsilon} = \Delta \boldsymbol{\varepsilon}_{el} + \Delta \boldsymbol{\varepsilon}_v + \Delta \boldsymbol{\varepsilon}_{ve}.$$

Detailed description of respective terms of Eq. (2.3) can be found, e.g., in [6–8].

### 3. *hp*-ADAPTIVE FEM

This section describes briefly the most important features of the *hp*-adaptive FEM, which we use to approximate solutions at both micro and macroscales. There are two main kinds of the adaptive finite element method:

- *h* type – based on a decrease of the element size and
- *p* type – based on a increase of the solution approximation order.

In our research we take advantage of the automatic version of *hp*-adaptive FEM. It was proposed and implemented into codes *hp2D* and *hp3D* by DEMKOWICZ *et al.* [12, 13]. Computation with these codes is performed as follows:

- an initial mesh is arbitrarily generated,
- reference solution is obtained on uniformly refined mesh with solution approximation order increased by one,
- the projection-based interpolation error estimate is computed and the most effective mesh refinement is performed,
- (possibly) anisotropic refinements are performed in order to generate the optimum mesh.

This approach provides both the fast convergence and solution error control.

As it was mentioned before, the *hp*-adaptive FEM is used in the proposed approach as a “coarse mesh generator”. It may also be used to obtain the fine mesh at the microscale.

## 4. LOCAL NUMERICAL HOMOGENIZATION

### 4.1. *An outline of the method*

Local numerical homogenization (LNH) was proposed by JHURANI [3, 9]. Implementations of this method can be also found in [10, 11]. We use this ap-

proach because neither, the separation of scales condition nor periodicity of the heterogeneous microstructure are required. Thus, the method is quite general. LNH is linked to the FEM, since neighboring scales are bridged using FEM discretizations.

As a first step, the two scales of analysis and the two meshes (coarse and fine) are determined. In order to generate the coarse mesh related to the macroscale we solve an auxiliary problem:

- the whole domain is treated as a homogeneous one (effective material properties are assumed on the basis of a simple method, e.g., mix rule),
- the auxiliary problem is solved using *hp*-adaptive FEM,
- coarse discretization with corresponding shape functions (possibly of higher order) is obtained.

The coarse mesh is optimal for the auxiliary problem and provides a reliable solution in a reasonable period of time. The actual problem will be solved using the same discretization. Accounting for the heterogeneous microstructure is performed for every coarse mesh element in the following way:

- within a coarse element the mesh is refined in order to fully comply with all of the inhomogeneities,
- fine mesh stiffness matrices and load vectors are assembled,
- effective stiffness matrices of coarse element calculated.

Such a procedure enables us to solve the problem of interest in a reliable way using coarse discretization instead of extremely fine one. It should be pointed out that the fine meshes for neighboring coarse elements do not need to be compatible. A scheme of the presented routine for a single coarse element is shown in Fig. 2.

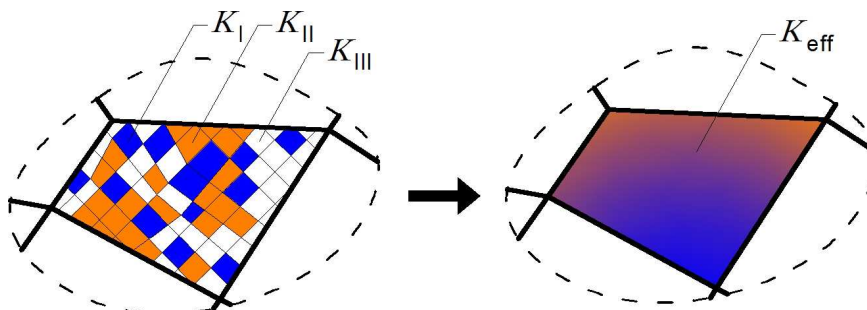


FIG. 2. Approach of local numerical homogenization.

Subsequently, coarse element stiffness matrices and respective load vectors are assembled. At last, the main problem can be solved using coarse discretization in a reasonable period of time.

#### 4.2. Calculation of the effective stiffness matrix

Details on the key part of the local numerical homogenization – calculation of the effective stiffness matrix – are given in [3] and are obtained by local method, i.e., for every coarse mesh element, difference of would-be solutions obtained using a single coarse element and a fine mesh based on its refinement, is minimized. Jhurani in his dissertation [3] posed this problem in a following form.

For a non-zero fine mesh load vector  $\mathbf{f}$ , known symmetric stiffness matrices for fine mesh elements assembled into  $\mathbf{K}$ , interpolation matrix  $\mathbf{A}$ , positive-definite symmetric weight matrix  $\mathbf{B}$ , dimensionless small parameter  $\epsilon > 0$ , we look for a symmetric matrix  $\widehat{\mathbf{K}}^\dagger$  that minimizes  $E$ , where:

$$(4.1) \quad E(\widehat{\mathbf{K}}^\dagger) = \frac{1}{2} \left\| (\mathbf{K}^\dagger - \mathbf{A} \widehat{\mathbf{K}}^\dagger \mathbf{A}^T) \mathbf{f} \right\|_{\mathbf{B}}^2 + \frac{\epsilon}{2} \left\| \mathbf{K}^\dagger - \mathbf{A} \widehat{\mathbf{K}}^\dagger \mathbf{A}^T \right\|_{F, \mathbf{B}}^2 \left\| \mathbf{f} \right\|_2^2$$

and  $\widehat{\mathbf{K}}$  – effective coarse element stiffness matrix,  $\widehat{\mathbf{K}}^\dagger$  – Moore-Penrose pseudoinverse of  $\widehat{\mathbf{K}}$ ,  $\|\mathbf{x}\|_2 = \sqrt{\text{trace}(\mathbf{x}^T \mathbf{x})}$  – Euclidean norm,  $\|\mathbf{x}\|_{\mathbf{B}} = \sqrt{\text{trace}(\mathbf{x}^T \mathbf{B} \mathbf{x})}$  – Euclidean norm weighted with  $\mathbf{B}$ ,  $\|\mathbf{X}\|_{F, \mathbf{B}} = \sqrt{\text{trace}(\mathbf{X}^T \mathbf{B} \mathbf{X})}$  – Frobenius norm weighted with  $\mathbf{B}$ .

The first term of Eq. (4.1) measures the error of the local solution for a given local load vector, whereas the second one is added for regularization purposes. Matrix  $\widehat{\mathbf{K}}^\dagger$  is subsequently pseudoinverted into  $\widehat{\mathbf{K}}$ .

The key point of above procedure is construction of a mapping for coarse element degrees of freedom (DOF) to fine mesh DOF (using matrix  $\mathbf{A}$ ) and calculation of the assembled fine mesh load vector  $\mathbf{f}$ . The latter is found in a following way:

- the auxiliary problem with assumed homogeneity is solved,
- strain ( $\boldsymbol{\varepsilon}$ ) and stress ( $\boldsymbol{\sigma}$ ) tensor fields are calculated,
- tractions  $\mathbf{t}$  are evaluated on the basis of the stress field at the edges or faces of the elements and respective normal vectors  $\mathbf{n}$  as

$$(4.2) \quad \mathbf{t} = \boldsymbol{\sigma} \mathbf{n},$$

- if needed, tractions are equilibrated,
- integrating tractions resulting from Eq. (4.2) along the fine mesh element edges or faces one obtains fine mesh load vector of the  $i$ -th element as:

$$(4.3) \quad \mathbf{f}^{el.i} = \int_{S_\sigma} \mathbf{v} \mathbf{t} ds,$$

- fine mesh load vectors calculated according to Eq. (4.3) and respective stiffness matrices are assembled.

## 5. NUMERICAL RESULTS

The first example was solved in plane strain state in elastic range. A rectangular domain ( $2 \times 1$ ) shown in Fig. 3 was discretized with 2048 elements. Two phases with the volumetric fraction of 0.5 were assumed:

- “white” with  $E = 100$  and  $\nu = 0.3$  and
- “black” with  $E = 200$  and  $\nu = 0.3$ .

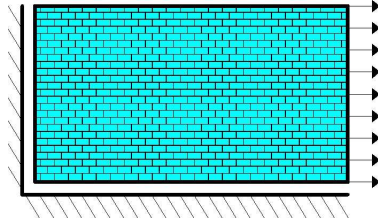


FIG. 3. Analyzed domain with homogenized material at macroscale.

The load intensity  $q$  is equal to 1. Three random material distribution cases are presented in Fig. 4. The number of degrees of freedom is equal to 4290 in each case. Subsequently, the whole domain was discretized with one coarse element with eight degrees of freedom. Horizontal displacements along the right-hand side edge for three distribution cases are shown in Fig. 5–7. Red solid line

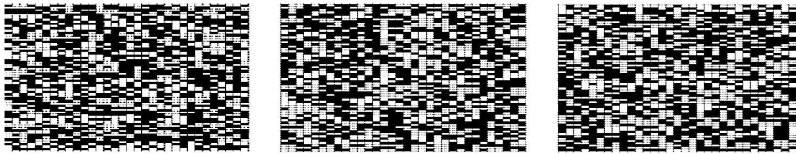


FIG. 4. Random material distribution cases.

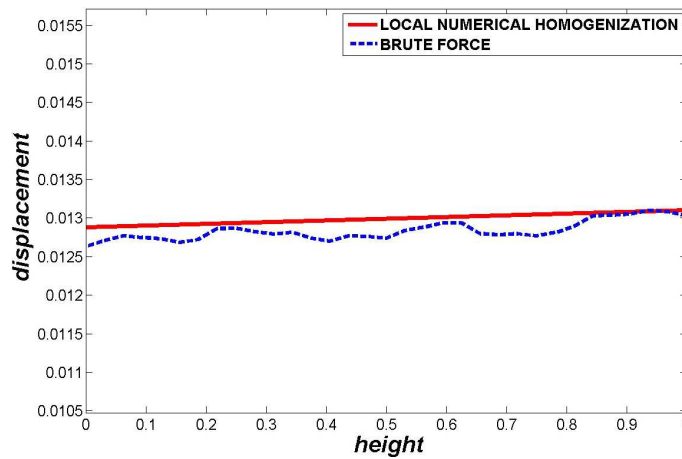


FIG. 5. Horizontal displacements – case I.

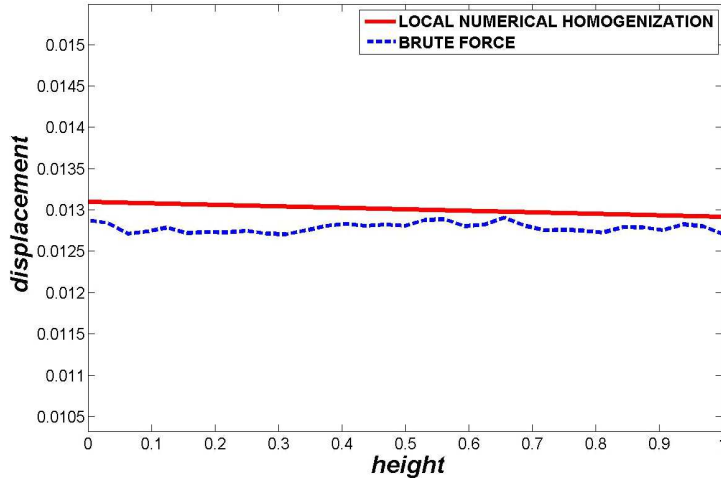


FIG. 6. Horizontal displacements – case II.

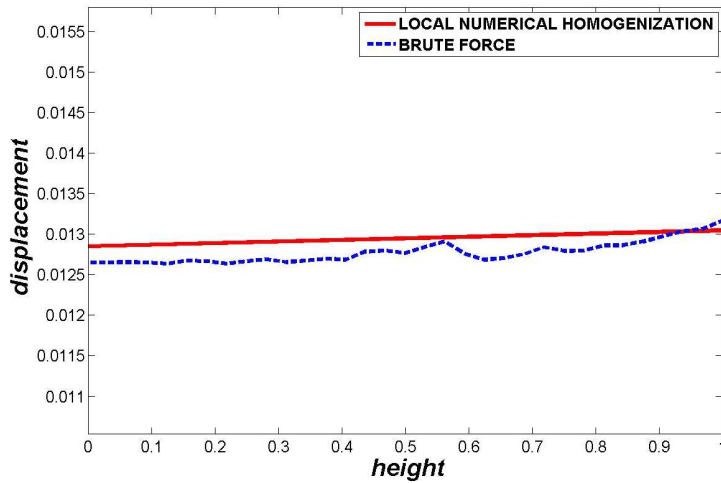


FIG. 7. Horizontal displacements – case III.

shows LNH solution, blue dashed curve shows the solution obtained using the fine mesh. Differences in solutions do not exceed 1 percent. Axis  $y$  limits in the graph are set to interval  $[0.9u_{\max}, 1.2u_{\max}]$ . Otherwise, the graphs of both solutions would be indistinguishable.

The domain analyzed in plane strain state is the next example presented in Fig. 8. The Burgers viscoelastic material model was used ( $E_{\text{white}} = 100$ ,  $E_{\text{black}} = 200$ , remaining parameters were assumed as the same for both phases, i.e.  $\nu_{el} = 0.3$ ,  $\nu_{ve} = 0.3$ ,  $\nu_v = 0.49$ ,  $\lambda_{ve} = 3.29e2$ ,  $\tau = 9.68e-6$ ,  $\lambda_{\infty} = 100$ ). The loading was applied in one step. Dimensions and load intensity were assumed as

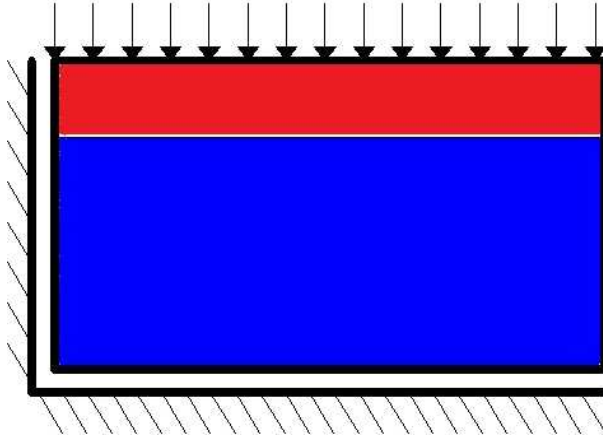


FIG. 8. The analyzed domain.

in the previous numerical example. Distribution of two phases is also random and their volumes are equal but their sizes are different in two layers. This is a typical situation in the case of asphalt pavement layers for example – neighboring layers are made of aggregate of different sizes.

Coarse mesh (a regular one) is shown in Fig. 9. It consists of 128 elements. Subsequently, it was refined within coarse elements as follows:

- the red layer elements were discretized with 144 fine elements,
- the blue layer elements were discretized with 36 fine elements.

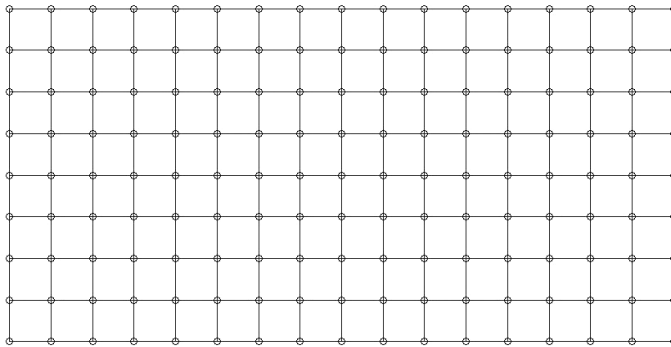


FIG. 9. Coarse mesh.

Globally the fine mesh is too dense to be presented. Zooming in, one can notice the incompatibility of the fine meshes within neighboring coarse elements (Fig. 10). Also the distribution of two phases is shown at the interface. Maps of both displacement components are presented in Fig. 11. The results demonstrate the potential of the proposed approach.

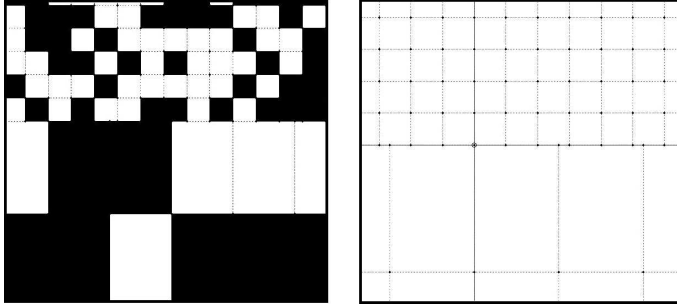


FIG. 10. Incompatibility of the fine meshes at the interface of layers.

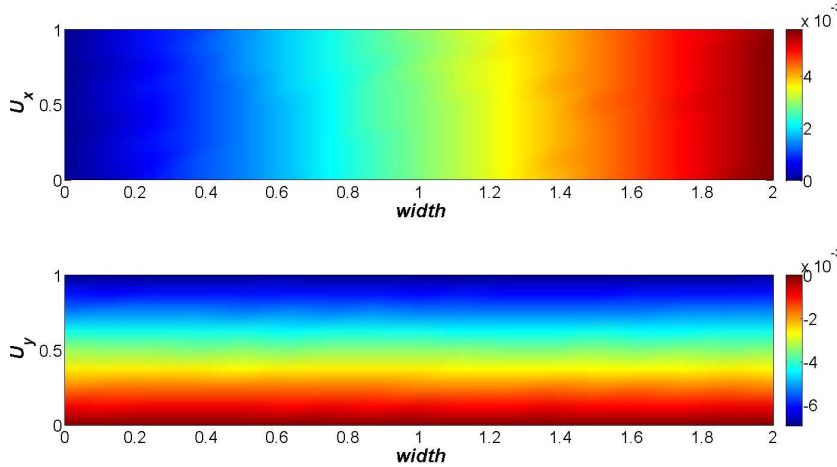


FIG. 11. Maps of the displacement component.

## 6. CONCLUSIONS

Preliminary tests on integration of the *hp*-adaptive FEM and local numerical homogenization were presented in this paper the obtained results are very promising. Advantages of the proposed approach are as follows:

- reasonable reduction of the number of DOF by introducing only negligible error to the solution for non-periodic and inelastic materials,
- significant decrease of the amount of computational cost,
- reliable solution of the problem, which could not be solved using the direct approach.

## ACKNOWLEDGMENT

This research was sponsored by the Polish National Science Center (NCN) under the project UMO-2011/01/B/ST6/07312.

## REFERENCES

1. GEERS M., KOUZNETSOVA V., BREKELMANS W., *Multi-scale first-order and second-order computational homogenization of microstructures towards continua*, International Journal for Multiscale Computational Engineering, **1**, 4, 371–386, 2003.
2. MANG H.A., AIGNER E., EBERHARDSTEINER J., HACKSPIEL C., HELLMICH CH., HOFSTETTER K., LACKNER R., PICHLER B., SCHEINER ST., STÜRZENBECHER R., *Computational multiscale analysis in civil engineering*, Interaction and Multiscale Mechanics, **2**, 2, 109–128, 2009.
3. JHURANI C.K., *Multiscale modeling using goal-oriented adaptivity and numerical homogenization*, PhD thesis, The University of Texas, Austin, 2009.
4. BENSOUSSAN A., LIONS J.L., PAPANICOLAOU G., *Asymptotic analysis for periodic structures*, North-Holland, Amsterdam, 1978.
5. WIĘCKOWSKI Z., *Dual finite element methods in homogenization for elastic-plastic fibrous composite material*, Int. J. Plasticity, **16**, 199–221, 2000.
6. COLLOP A.C., SCARPAS A.T., KASBERGEN C., DE BONDT A., *Development and finite element implementation of a stress dependent elasto-visco-plastic constitutive model with damage for asphalt*, Transportation Research Record 1832, 96–104, Washington D.C., 2003.
7. WOLDEKIDAN M.F., *Response modeling of bitumen, bituminous mastic and mortar*, PhD thesis, Technische Universiteit Delft, 2011.
8. WOLDEKIDAN M.F., HUURMAN M., VACCARI E., POOT M., *Meso mechanical analysis of asphalt concrete response*, Proceedings of the International Symposium on Heavy Duty Asphalt Pavements and Bridge Deck Pavements, ISAP, China, 2012.
9. JHURANI C.K., DEMKOWICZ L., *ICES Reports 09-34÷09-36*, The University of Texas, Austin, 2009.
10. KLIMCZAK M., CECOT W., *Local homogenization in modeling of asphalt pavement structures*, Technical Transactions, **3**, 1-B/2011, 87–94, 2011.
11. KLIMCZAK M., CECOT W., *Local numerical homogenization in modeling of heterogeneous visco-elastic materials*, Computer Methods in Materials Science, **13**, 2, 226–230, 2013.
12. DEMKOWICZ L., *Computing with hp-Adaptive Finite Element Method, Vol. 1: One and Two Dimensional Elliptic and Maxwell Problems*, Chapman and Hall, 2006.
13. DEMKOWICZ L., KURTZ J., PARDO D., PASZYNSKI M., RACHOWICZ W., ZDUNEK A., *Computing with hp-Adaptive Finite Element Method, Vol. 2: Frontiers Three Dimensional Elliptic and Maxwell Problems with Applications*, Chapman and Hall, 2007.

*Received June 30, 2014; accepted January 14, 2015.*

---